STRESS CONCENTRATION IN A RUBBER SHEET UNDER AXIALLY SYMMETRIC STRETCHING

by

W. H. Yang

GALCIT SM 66-16

DECEMBER 1966

National Aeronautics and Space Administration

Research Grant No. NsG-172-60

GALCIT 120

Firestone Flight Sciences Laboratory

Graduate Aeronautical Laboratories

California Institute of Technology

Pasadena, California

[redacted]

STRESS CONCENTRATION IN A RUBBER SHEET UNDER AXIALLY SYMMETRIC STRETCHING*

Wei Hsuin Yang
Assistant Professor
Department of Engineering Mechanics
The University of Michigan

ABSTRACT

A class of axially symmetric problems concerning a highly elastic circular rubber sheet with: (1) a centered circular hole or (2) a rigid circular inclusion under outward radial loading at outer boundary, and (3) a rigid outer boundary and a concentric hole under inward radial loading around the hole are solved. The differential equation governing the deformation is formulated under the assumptions of plane stress and incompressible, initially isotropic material and is integrated in the plane of principal stretch ratios.

* This work was supported in part by NASA Research Grant NsG-172-60, through the California Institute of Technology

[redacted]

INTRODUCTION

Among various theories of non-linear elasticity, a well known one is presented comprehensively by Green and Zerna [1]. The framework of this theory is based on the Cauchy-Green type of tensorial strain measure and the constitutive relation expressed by a strain energy density function which is a function of the strain invariants. A special case of the theory is for the incompressible materials.

On the basis of this special case, the axially symmetrical deformations in the plane of a thin rubber sheet are reformulated in this paper in terms of a second order non-linear differential equation governing the deformation. The solutions are obtained for three types of boundary conditions which correspond to the problems of a circular imperfection (a hole or a rigid inclusion) in the rubber sheet under outward radial stretching and the problem of a circular sheet fixed along outer boundary under inward radial stretching by forces applied along the boundary of a center hole as shown in Fig. 1 (a, b, c). The results reveal some interesting feather of stress concentration under large elastic deformations.

Rivlin and Thomas [2] have analyzed the strain distribution around a hole in a sheet under axially symmetrical deformation, however, given no results on stress concentration. Their numerical solution is obtained by a forward integration method. The results in their paper have been computed for the sheet with radius three times greater than the radius of the hole in the undeformed state. In order to obtain the solution for an infinitely large sheet (or a very small hole in a large sheet), the integration has range from the radius of the hole to infinity. In this case, their method proves inefficient and error-accumulating after integrating over a large distance. Since their integration started from the boundary of the hole, they have specified the boundary conditions at the hole to consist both stress free condition and a given hole expansion ratio. The stress applied at the outer boundary necessary to produce the deformation is then a computed quantity. For their problem, the stress at the outer boundary is usually prescribed which determines the hole expansion ratio. In this circumstance, their integration procedure is an inverse one which requires a correct guess on the hole expansion ratio in order to satisfy the prescribed condition on the outer boundary.

To resolve the problem arised from an infinite sheet, the variables in the differential equation are transformed into a new set of variables namely the principal stretch ratios in the radial and circumferential directions. The differential equation reduces to a first order one. Since the stretch ratios are bounded, the integration of the differential equation is always over a finite region even for an infinitely large sheet. In the plane of the principal stretch ratios, the direction of integration can be conveniently chosen for either increasing or decreasing independent variable, depending on the described boundary conditions.

The numerical solutions are presented for all three types of problems with the strain energy density function suggested by Mooney [3] which has the form

$$W(I_1, I_2) = C_1(I_1 - 3) + C_2(I_2 - 3)$$
$$= C_1[(I_1 - 3) + \alpha(I_2 - 3)] \qquad (1)$$

where I_1, I_2 are strain invariants and C_1, C_2 are material constants with dimension of force per unit area and $\alpha = C_2/C_1$. Various quantities of interest are presented graphically.

The neo-Hookean material is a special case when α is equal to zero. For this material, the differential equation is in a simpler form. Several close form approximate solutions are obtained for various regions in the sheet by solving the non-linear integral equation in the later section of approximate solutions.

ANALYSIS

For a thin sheet with dimensions of the hole or inclusion much greater than its thickness, the plane stress assumption should lead to a good approximation. By symmetry of the problem, the cylindrical coordinate with origin at the center of the hole or inclusion is employed. The deformations under consideration are described by the mapping

$$\rho = \rho(r)$$
$$\Theta = \theta \qquad (2)$$
$$\eta = z\lambda_3(r)$$

where (ρ, Θ, η) and (r, θ, z) are deformed and undeformed coordinates respectively. The principal stretch ratios in the radial and circumferential directions are respectively

$$\lambda_1 = \rho' = \frac{d}{dr}(\rho)$$
$$\lambda_2 = \rho/r \tag{3}$$

and the stretch ratio in the z direction is

$$\lambda_3 = \frac{r}{\rho\rho'} \tag{4}$$

as a result of incompressible material for which $\lambda_1 \lambda_2 \lambda_3 = 1$.

The strain invariants are

$$I_1 = \lambda_1^2 + \lambda_2^2 + \lambda_3^2$$
$$I_2 = \lambda_1^{-2} + \lambda_2^{-2} + \lambda_3^{-2} \tag{5}$$
$$I_3 = 1$$

The non-zero stress components measured per unit deformed area are given by [2]

$$t_1 = 2(\lambda_1^2 - \lambda_3^2)\left(\frac{\partial W}{\partial I_1} + \lambda_2^2 \frac{\partial W}{\partial I_2}\right)$$

$$t_2 = 2(\lambda_2^2 - \lambda_3^2)\left(\frac{\partial W}{\partial I_1} + \lambda_1^2 \frac{\partial W}{\partial I_2}\right) \tag{6}$$

in the radial and circumferential directions respectively.

The resultants of these stresses measured per unit length along the circumference in the respective directions are

$$T_1 = 2h\lambda_3 (\lambda_1^2 - \lambda_3^2)\left(\frac{\partial W}{\partial I_1} + \lambda_2^2 \frac{\partial W}{\partial I_2}\right)$$

$$T_2 = 2h\lambda_3 (\lambda_2^2 - \lambda_3^2)\left(\frac{\partial W}{\partial I_1} + \lambda_1^2 \frac{\partial W}{\partial I_2}\right) \tag{7}$$

where h is the thickness of the sheet in the undeformed state. These stress resultants must satisfy the equations of equilibrium. Two of the equations are automatically satisfied. The equation in the radial direction, without the presence of body forces, takes the form

$$\frac{d}{d\rho}(\rho\ T_1) = T_2 \tag{8}$$

in the deformed coordinate. Expressing it in terms of undeformed coordinate, equation (8) becomes

$$\frac{d}{dr}(\rho\ T_1) = \rho'\ T_2 \tag{9}$$

Substituting equation (7), (4), (3) and (1) into equation (9), the differential equation governing $\rho(r)$ is obtained as follows

$$\rho' - \frac{3r^2}{\rho^2 \rho'^3} + \frac{3r^3}{\rho^3 \rho'^2} + r\rho'' + \frac{3r^3 \rho''}{\rho^2 \rho'^4} - \frac{\rho}{r}$$

$$+ \alpha \left\{ \frac{\rho^2 \rho''}{r} - \frac{1}{\rho'^3} + \frac{3r\rho''}{\rho'^4} + \frac{\rho \rho'^2}{r} - \frac{\rho^2 \rho'}{r^2} + \frac{r^3}{\rho^3} \right\} = 0 \tag{10}$$

By the use of equation (3), the differential equation is reduced to a first order one

$$\frac{d\lambda_1}{d\lambda_2} = - \frac{\lambda_1}{\lambda_2} \frac{3 + \lambda_1^3 \lambda_2^3 + \alpha(\lambda_1^2 + \lambda_2^2 + \lambda_1 \lambda_2 + \lambda_1^4 \lambda_2^4)}{3 + \lambda_1^4 \lambda_2^2 + \alpha(3\lambda_2^2 + \lambda_1^4 \lambda_2^4)} \tag{11}$$

with the companion equation

$$\frac{d\lambda_2}{\lambda_1 - \lambda_2} = \frac{dr}{r} \tag{12}$$

After solving equation (11) for a given boundary condition, the solution of the form

$$\lambda_1 = \lambda_1(\lambda_2) \tag{13}$$

can be used for the integration of equation (12), giving the relation of λ_2 and r. Thus, the relation of ρ and r is determined which is the solution to equation (10).

Equation (11) has no singularity. It can be integrated easily by any numerical procedure for initial value problems in ordinary differential equation. A commonly used one is the Runge-Kutta method [4]. The error of this procedure is of $0(\delta^5)$ where δ is the increment of integration.

Since λ_1 and λ_2 are non-negative, the solution of equation (11) lies in the first quadrant of $\lambda_1 - \lambda_2$ plane. There are four special curves in this quadrant representing the solutions: (1) on the boundary of the hole. (2) at infinity. (3) on the boundary of the rigid inclusion and a fixed boundary. (4) on a circle in the rubber sheet where t_2 vanishes. These curves are shown in Fig. 2 and labelled accordingly.

The condition on the hole is $t_1 = 0$ which gives the curve (1), $\lambda_1 = \lambda_2^{-1/2}$. At infinity $\lambda_1 = \lambda_2$ which is the curve (2). For a fixed boundary ρ equals r which gives the curve (3), $\lambda_2 = 1$. $t_2 = 0$ yields $\lambda_1 = \lambda_2^{-2}$ which is the curve (4). The solutions in the region between curves (1) and (2) describe the problem of a hole in the sheet under outward stretching. The solutions in the region between curves (2) and (3) describe the problem of a rigid inclusion in the sheet under outward stretching. Between curves (3) and (4), there exist solutions of a circular sheet with fixed outer boundary under inward stretching forces applied around a center hole. This can be done also by considering a circular sheet with fixed outer boundary being pulled downward at the center through a frictionless small ring as shown in Fig. 3. The solutions on the left side of curve (4), where $\lambda_1 < \lambda_2^{-2}$, give negative t_2. Since a thin rubber sheet has practically no resistance to in-plane compression, the plane stress formulation ceases to describe this phenomenon. Physically, the sheet is wrinkled in such a region. There, fore, the curve (4) also gives the boundaries of wrinkled zone.

The integration of equation (11) can start from any point in the first quadrant of $\lambda_1 - \lambda_2$ plane, however, the starting point is usually on one of the four curves where boundary conditions are given. The integration can be made in either direction (increasing or decreasing direction of λ_2). If a check on the accuracy is desired, a round trip integration can be made. The results shown in Fig. 2 have been obtained in this manner. The error introduced after a round trip integration with increment $\delta = 0.01$ is beyond the description of an eight-place decimal number.

The solutions of equation (11) already provide the information of stress and strain concentrations for all the problems considered. For information on the deformations, further integrations of equation (12) is required.

The results for various quantities of interest are shown in the later section of numerical results.

APPROXIMATE SOLUTIONS

For neo-Hookean material ($\alpha = 0$), equation (11) reduces to the simpler form

$$\frac{d\lambda_1}{d\lambda_2} = -\frac{\lambda_1}{\lambda_2}\,\frac{3+\lambda_1^3\lambda_2^3}{3+\lambda_1^4\lambda_2^2} = F(\lambda_1, \lambda_2) \tag{14}$$

This differential equation can be changed to a non-linear integral equation of the form

$$\lambda_1(\lambda_2) = \lambda_1(\lambda_o) + \int_{\lambda_o}^{\lambda_2} F[\lambda_1(\zeta), \zeta]\, d\zeta \tag{15}$$

where λ_o is a constant value of λ_2 in the domain of solutions discussed in the previous section.

The solutions of equation (15) can be obtained by the method of successive approximations,

$$\lambda_1^{(n+1)}(\lambda_2) = \lambda_1^{(n)}(\lambda_o) + \int_{\lambda_o}^{\lambda_2} F[\lambda_1^{(n)}(\zeta), \zeta]\, d\zeta \qquad n = 0, 1, 2 \ldots \tag{16}$$

The convergence conditions for this process are given by Tricomi [5]. The function F in equation (15) satisfies those conditions. In principle, uniformly valid solutions can be obtained by successive approximations.

For higher order approximations however, the integrations involve algebraic complications.

If we can choose a zeroth order approximation close to the exact solution in some region then the first order approximation will be accurate at least in that region. The approximate solutions are obtained in this manner for regions near the boundaries of the three types of problems.

For the region near the hole, the zeroth order approximation is chosen as

$$\lambda_1^{(o)}(\lambda_2) = \frac{1}{\sqrt{\lambda_2}} \tag{17}$$

The first order approximation

$$\lambda_1^{(1)}(\lambda_2) = \frac{1}{2}\left(\frac{3}{\sqrt{\lambda_2}} - \frac{1}{\sqrt{\lambda_h}}\right) + \frac{1}{4}(\lambda_h - \lambda_2) \tag{18}$$

is obtained from equation (16), where λ_h is a value of λ_2 on the boundary of the hole.

In the region corresponding to the large value of r, a zeroth order approximation can be chosen as

$$\lambda_1^{(0)}(\lambda_2) = \lambda_2 \tag{19}$$

The first order approximation is

$$\lambda_1^{(1)}(\lambda_2) = 2\lambda_\infty - \lambda_2 \tag{20}$$

where λ_∞ is a value of λ_2 at $r = \infty$.

For the regions near a fixed boundary and near the boundary of the wrinkle zone, the values of $d\lambda_1/d\lambda_2$ become large. λ_1 is very sensitive to the variation of λ_2. It is desirable to interchange the dependent and independent variables in equation (14). This leads to the integral equation

$$\lambda_2(\lambda_1) = \lambda_2(\lambda_o) + \int_{\lambda_o}^{\lambda_1} F^{-1}[\ \zeta,\ \lambda_2(\ \zeta\ )\ ]\ d\zeta \tag{21}$$

where λ_o here is a constant value of λ_1.

For the region near a fixed boundary, a zeroth order approximation is taken as

$$\lambda_2^{(o)}(\lambda_1) = 1 \tag{22}$$

which gives the first order approximation

$$\lambda_2^{(1)}(\lambda_1) = 1 + \lambda_f - \lambda_1 + \ln\left\{\frac{\lambda_f}{\lambda_1}\left(\frac{3+\lambda_1^3}{3+\lambda_f^3}\right)^{1/3}\left(\frac{k+\lambda_1}{k+\lambda_f}\sqrt{\frac{k^2-k\lambda_f+\lambda_f^2}{k^2-k\lambda_1+\lambda_1^2}}\right)^{k^{-2}}\right\}$$

$$+ k^{-1/2}\tan^{-1}\frac{\sqrt{3}k(\lambda_1-\lambda_f)}{2k^2-k(\lambda_1+\lambda_f)+2\lambda_1\lambda_f} \tag{23}$$

where $k=3^{1/3}$.

where λ_f is a value of λ_1 on the fixed boundary.

For the region near the boundary of wrinkle zone, a zeroth order approximation is chosen as

$$\lambda_2^{(o)}(\lambda_1) = \frac{1}{\sqrt{\lambda_1}} \tag{24}$$

The first order approximation

$$\lambda_2^{(1)}(\lambda_1) = \lambda_w - \lambda_1 + \frac{2}{\sqrt{\lambda_1}} - \frac{1}{\sqrt{\lambda_w}} + \frac{8}{3k} \ln\left(\frac{k+\lambda_w}{k+\lambda_1}\sqrt{\frac{k^2-k\lambda_1+\lambda_1^2}{k^2-k\lambda_w+\lambda_w^2}}\right)$$

$$+ 8\sqrt{3}\tan^{-1}\frac{\sqrt{3}k(\lambda_1-\lambda_w)}{2k^2-k(\lambda_1+\lambda_w)+2\lambda_1\lambda_w} \tag{25}$$

is obtained where λ_w is a value of λ_1 on the boundary of wrinkle zone.

These approximate solutions are plotted in Fig. 4 with the accurate numerical solutions. The results show that regions of validity for the approximate solutions are quite large.

The classical elasticity solutions are contained in a small region where $\lambda_1 \approx 1$, $\lambda_2 \approx 1$. The solution in the $\lambda_1 - \lambda_2$ plane is

$$\lambda_1(\lambda_2) = 2\lambda_\infty - \lambda_2 \tag{26}$$

Substituting equation (26) into equation (12) and integrating, the deformation function

$$\rho(r) = \lambda_{\infty} r + \frac{C}{r} \tag{27}$$

for classical elasticity is recovered where C is a constant of integration.

NUMERICAL RESULTS

The numerical solutions are presented in this section for a hole or a rigid inclusion of radius a in the rubber sheet under outward stretching at infinity. Three values of stretch ratios at infinity are taken as $\lambda_{\infty} = 1.25$, 1.7 and 2.1.

The deformations are shown in Fig. 5 (a, b). The solutions are also extended to the problem of a circular sheet of radius a with fixed outer boundary under inward stretching. The solutions for this problem are terminated at an envelop where t_2 changed sign from positive to negative.

The strain invariants $I_1(r)$ and $I_2(r)$ are shown in Fig. 6 and Fig. 7 respectively. The strain energy density function W(r) are shown in Fig. 8.

For the case of the hole, the results shown are in good agreement (for $1 \leq \frac{r}{a} \leq 3$) with the numerical solutions obtained by Rivlin and Thomas [2]. The results for larger values of r are varified by the experiments of Chu [6]. For very large value of r, the results approach the exact solution of a sheet without imperfection.

The stress concentration factors at the boundaries of the hole and the rigid inclusion are defined as

$$K_t^{(1)} = t_2(a)/t_1(\infty)$$

$$K_t^{(2)} = t_1(a)/t_1(\infty) \tag{28}$$

respectively. The corresponding strain concentration factors are defined as

$$K_\epsilon^{(1)} = [\lambda_2(a) - 1]/[\lambda_\infty - 1]$$

$$K_\epsilon^{(2)} = [\lambda_1(a) - 1]/[\lambda_\infty - 1] \tag{29}$$

These factors are plotted in Fig. 9 (a, b) as functions of applied stress or stretch ratio at infinity.

CONCLUSION

Under the nonlinear elasticity theory, the stress concentration character depends not only on the shape of the imperfection and the type of loading but the magnitude of the loading as well. The nonlinear behavior of stress concentration are contributed from both nonlinear constitutive relation and effects of large deformation. Physically, a softening type stress-strain relation should decrease stress concentration while a stiffening type should increase it. Geometrically, there are two types of effects from large deformation. One is from the change of shape, for example, a circular hole may be deformed to an ellipse like hole under certain deformation. The other effect is due to the change of thickness for some cross-section. Only the latter, which causes the redistribution of stresses over the deformed area, enters the problems under present consideration. There is no change of shape because of the symmetry of the problems.

The stress and strain concentration factors, under these non-linear influences, are increasing with the increasing load for the Mooney material. These factors should depend also on the value of α. This can be seen by the comparison of solutions in Fig. 2 and Fig. 4. The difference of solutions between the cases $\alpha = 0$ and $\alpha = 0.1$ is more substancial when higher stretch ratio are prescribed at infinity.

ACKNOWLEDGEMENT

The author wishes to express thanks to Mr. Kuo-Hsuin Hsu for his computation work.

LIST OF FIGURES

REFERENCES

1. Green, A. E. and Zerna, W., "Theoretical Elasticity," The Clarendon Press, Oxford, 1954.

2. Rivlin, R. S. and Thomas, A. G., "Large Elastic Deformations of Isotropic Materials VIII. Strain Distribution Around a Hole in a Sheet," Phil. Trans. A. 243, 1951, pp. 289-298.

3. Mooney, M., J. Appl. Phys., Vol. 11, 1940, p. 582.

4. Davis, H. T., "Introduction to Nonlinear Differential and Integral Equations," 1962, Dover edition, pp. 482-286.

5. Tricomi, F. G., "Integral Equations," 1957, Interscience, pp. 197-212.

6. Chu, B., GALCIT Report SM 65-21, August 1965, Graduate Aeronautical Laboratory, California Institute of Technology.

Fig

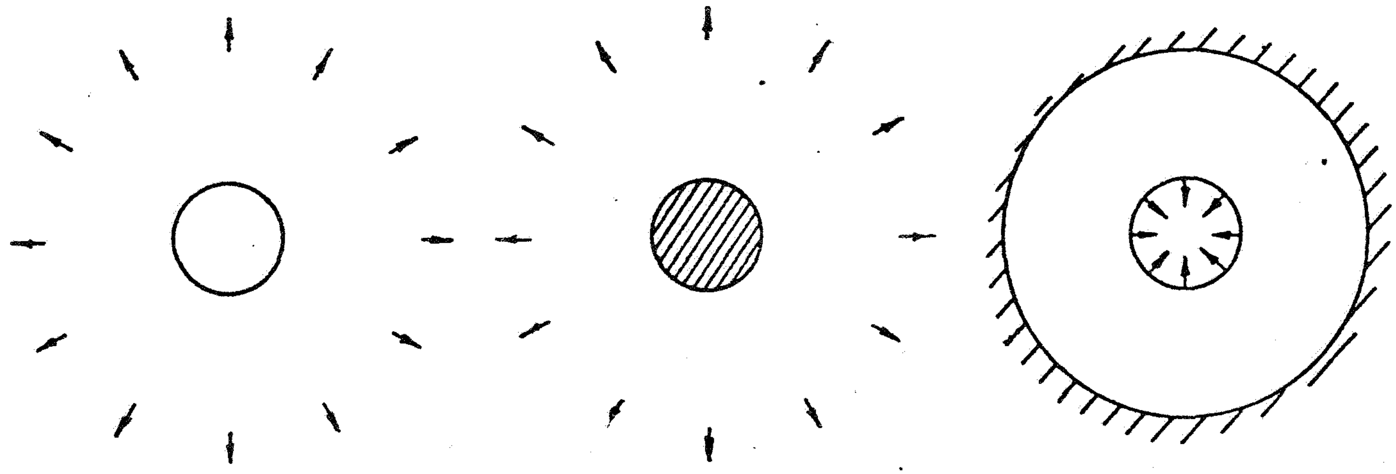

(a) Hole (b) Inclusion (c) Bounded Sheet

Fig

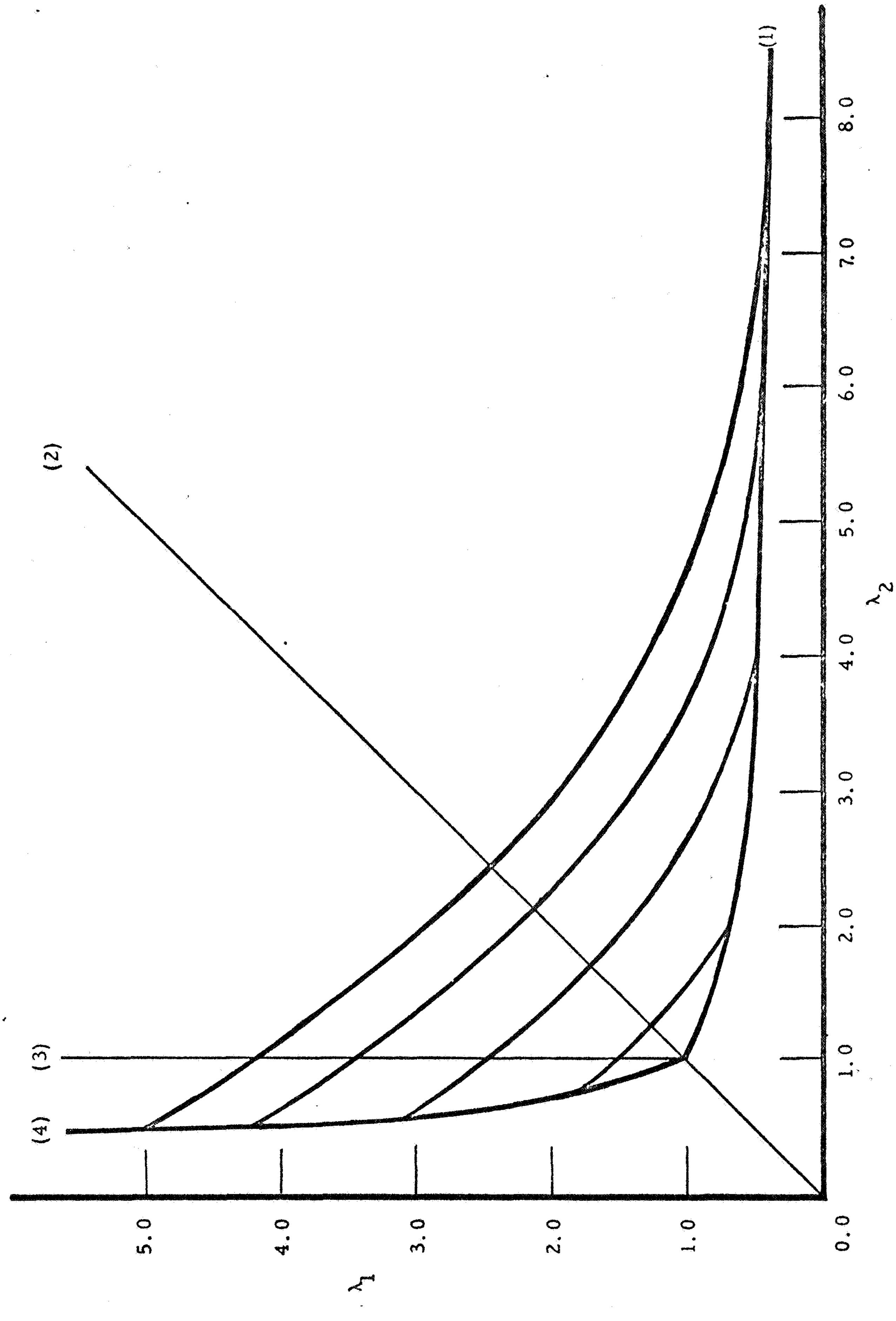

Fig

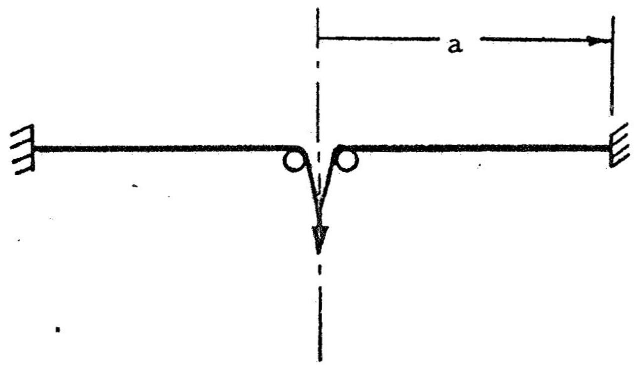

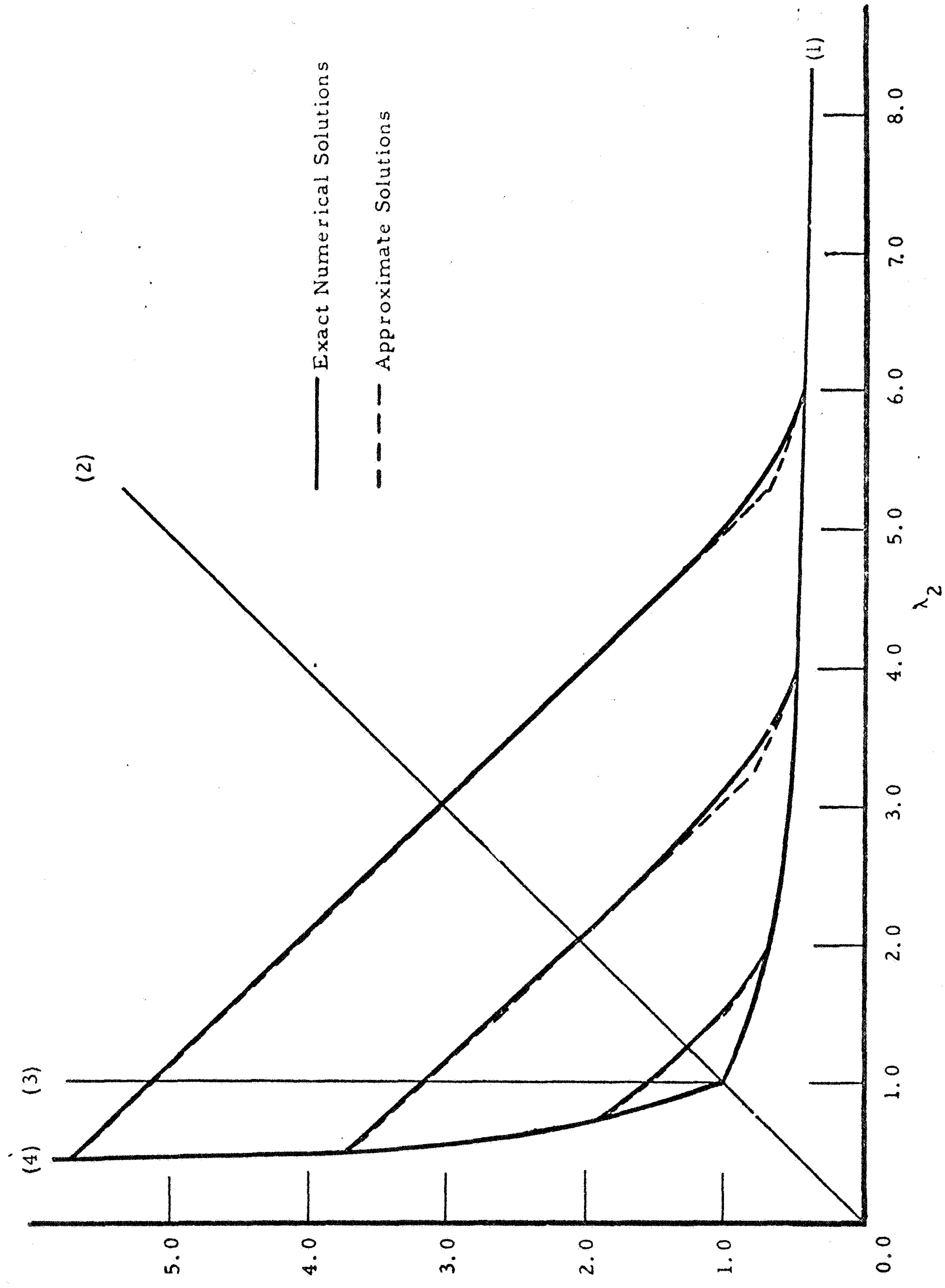
Exact Numerical Solutions
Approximate Solutions
(1)
(2)
(3)
(4)
0.0
1.0
2.0
3.0
4.0
5.0
6.0
7.0
8.0
λ_2

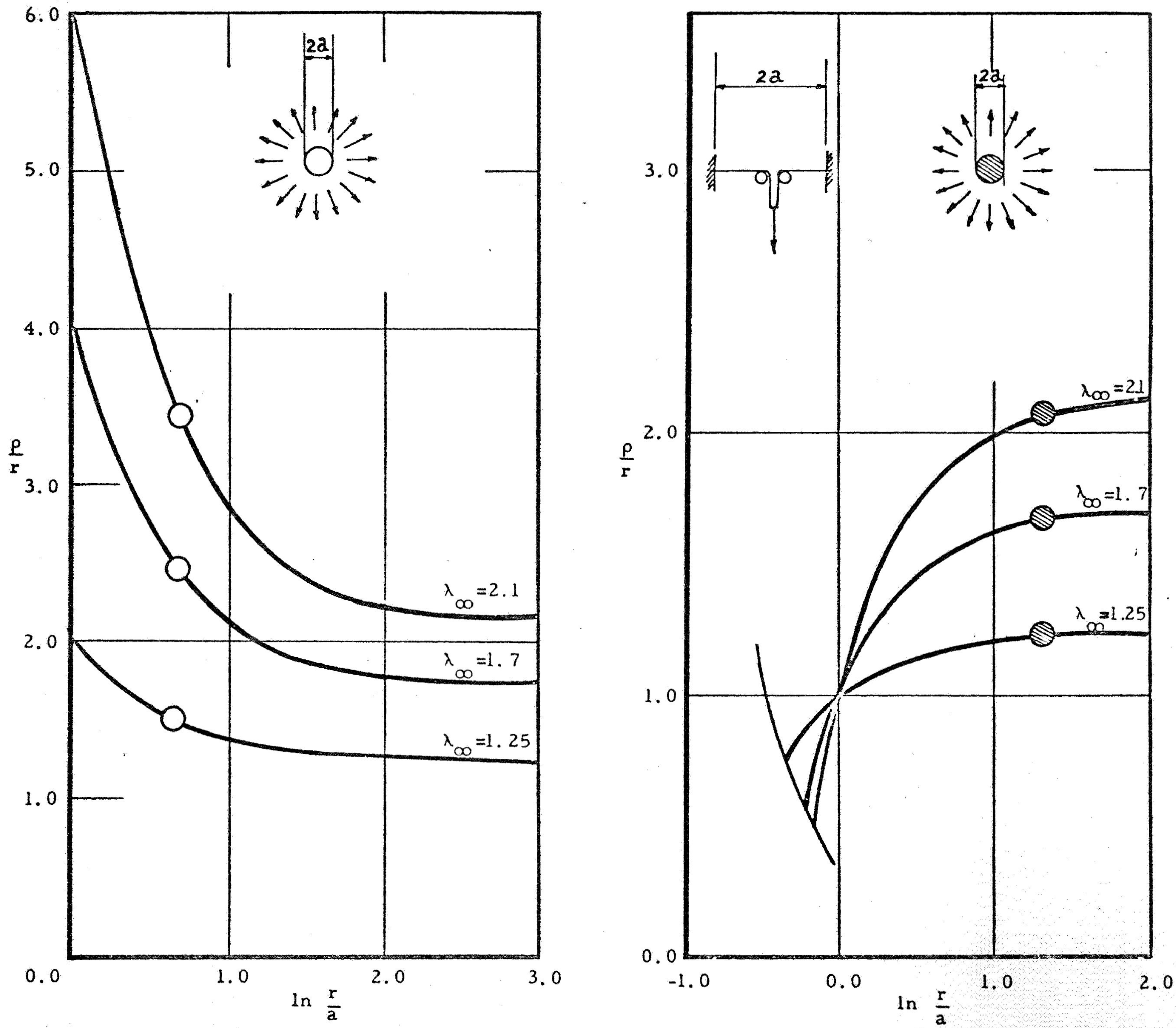

2a
λ_∞=2.1
λ_∞=1.7
λ_∞=1.25
$\frac{\rho}{r}$
ln $\frac{r}{a}$
2a
2a
λ_∞=2.1
λ_∞=1.7
λ_∞=1.25
$\frac{\rho}{r}$
ln $\frac{r}{a}$

Fig 5

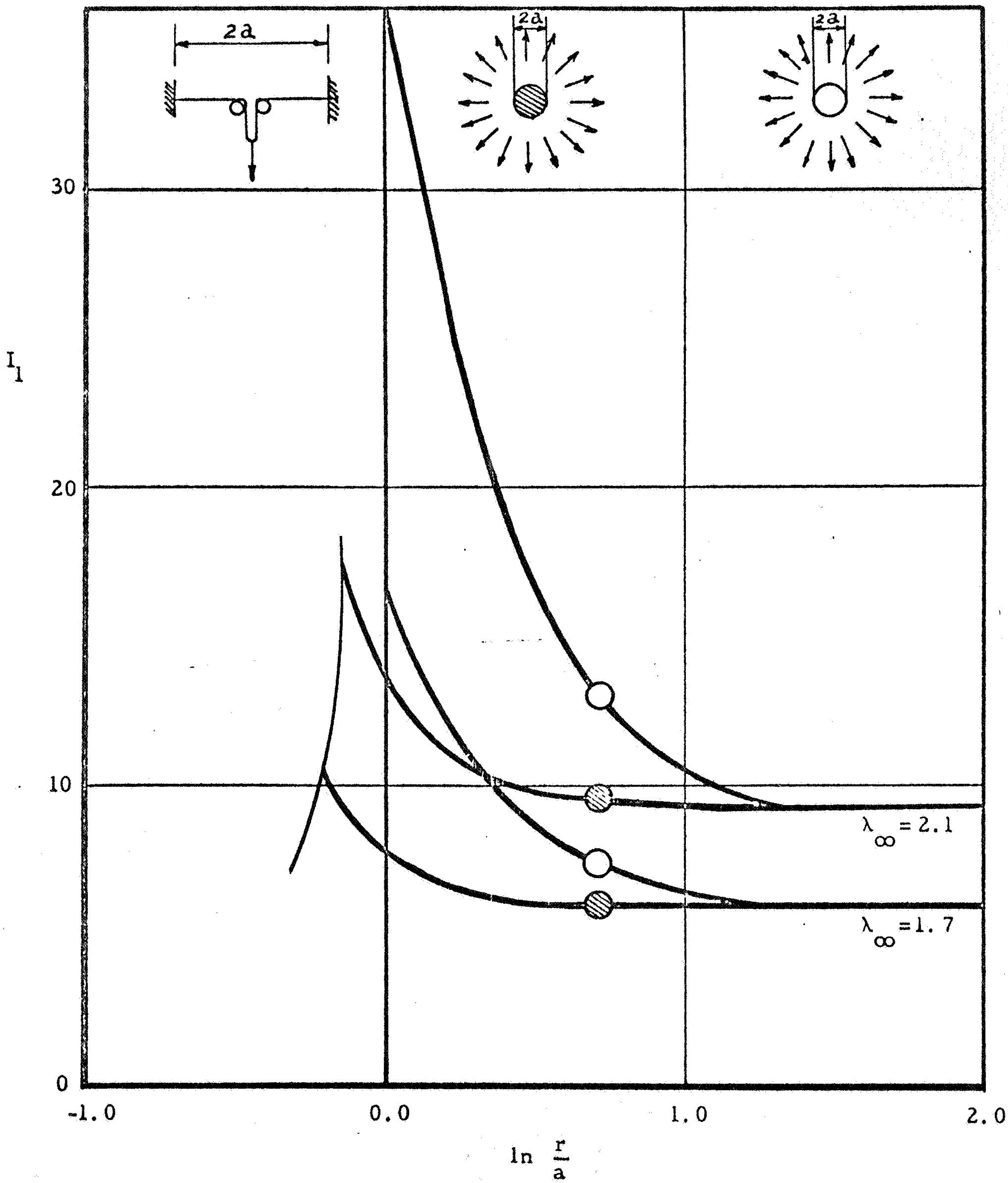
2a
2a
2a
30
20
10
0
I_1
$\lambda_\infty = 2.1$
$\lambda_\infty = 1.7$
-1.0
0.0
1.0
2.0
$\ln \frac{r}{a}$

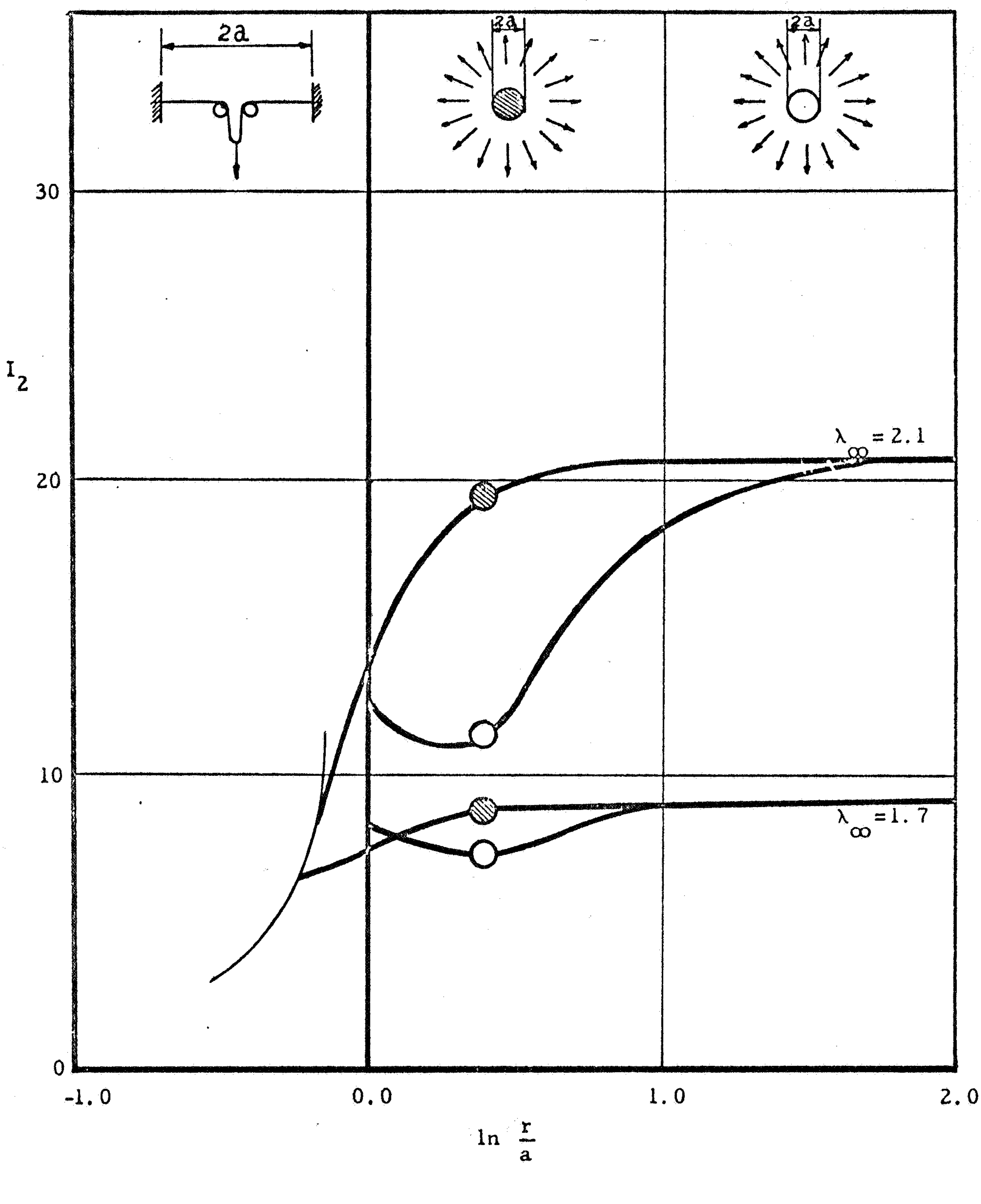
2a
2a
2a
30
20
10
0
I_2
$\lambda_\infty = 2.1$
$\lambda_\infty = 1.7$
-1.0
0.0
1.0
2.0
$\ln \frac{r}{a}$

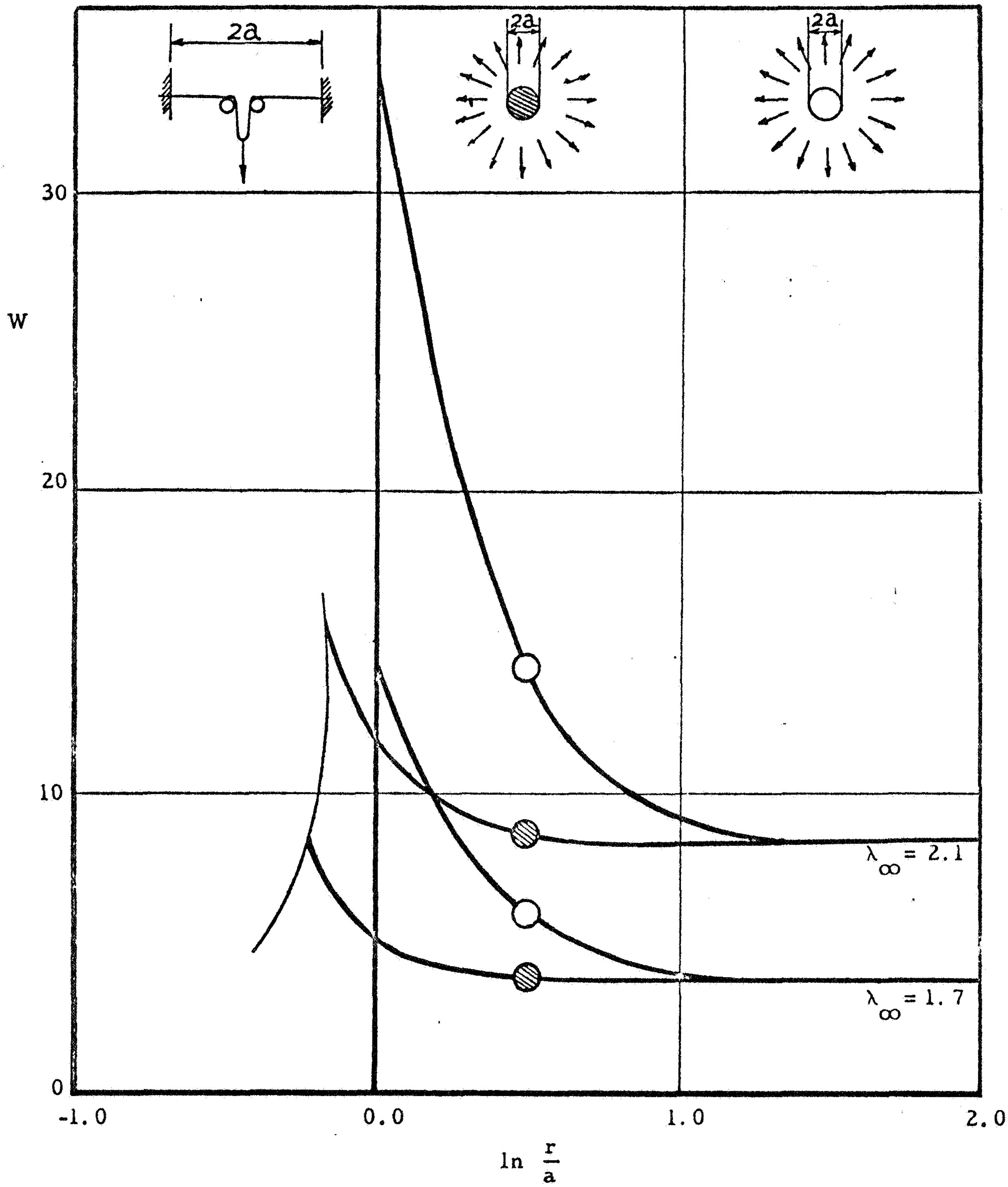
2a
2a
2a
30
20
10
0
W
λ∞ = 2.1
λ∞ = 1.7
-1.0
0.0
1.0
2.0
ln r/a

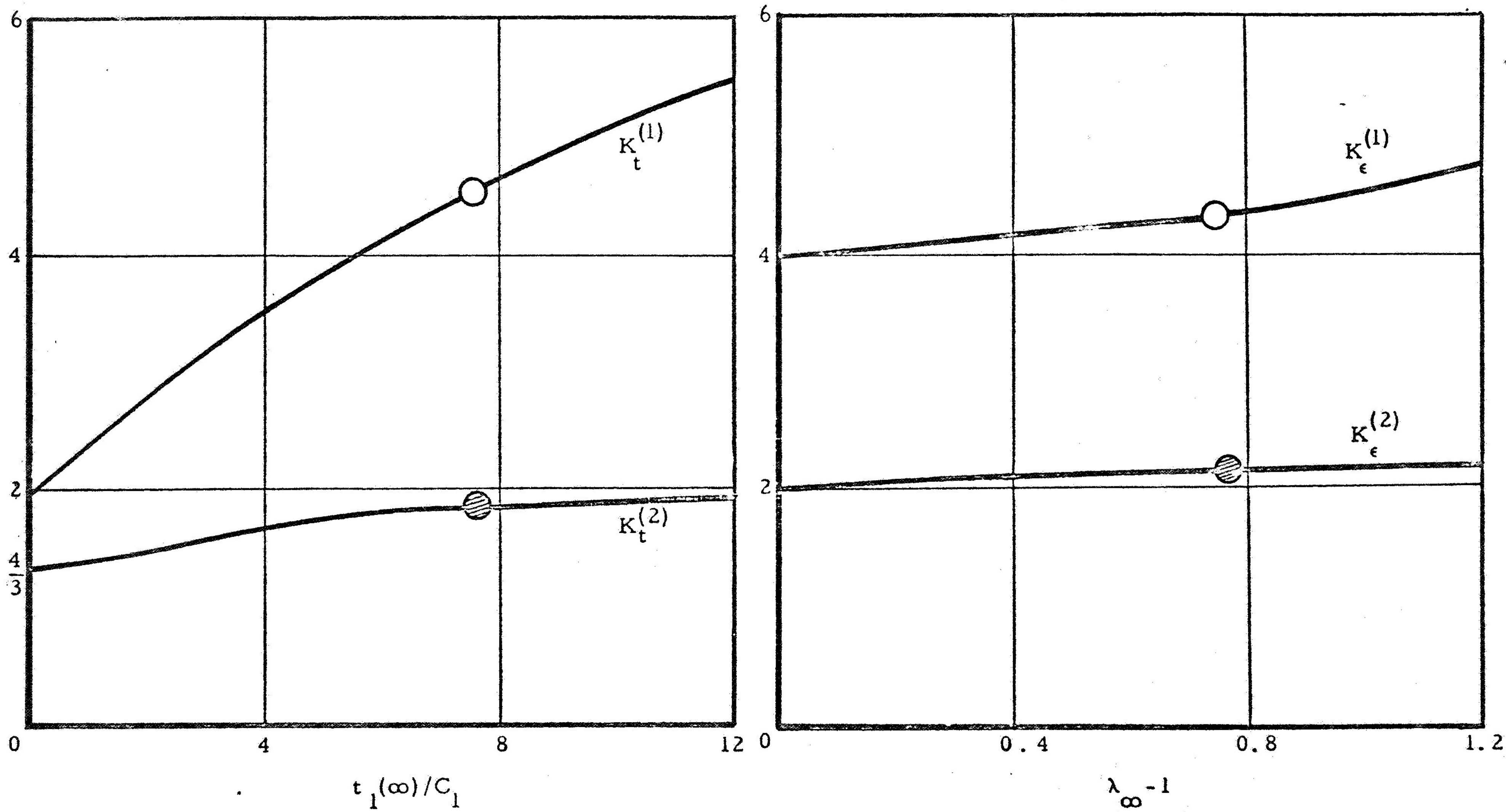

(a) Stress Concentration (b) Strain Concentration

Fig9